Recombinant modified vaccinia virus Ankara generating Ebola virus-like particles

Schweneker, Marc ; Laimbacher, Andrea S ; Zimmer, Gert ; Wagner, Susanne ; Schraner, Elisabeth M ; Wolferstätter, Michael ; Klingenberg, Marieken ; Dirmeier, Ulrike ; Steigerwald, Robin ; Lauterbach, Henning ; Hochrein, Hubertus ; Chaplin, Paul ; Suter, Mark ; Hausmann, Jürgen

Abstract: There are currently no approved therapeutics or vaccines to treat or protect against the severe hemorrhagic fever and death caused by Ebola virus (EBOV). Ebola virus-like particles (EBOV VLPs) consisting of the matrix protein VP40, the glycoprotein (GP), and the nucleoprotein (NP) are highly immunogenic and protective in nonhuman primates against Ebola virus disease (EVD). We have constructed a modified vaccinia virus Ankara-Bavarian Nordic (MVA-BN) recombinant coexpressing VP40 and GP of EBOV Mayinga and the NP of Taï Forest virus (TAFV) (MVA-BN-EBOV-VLP) to launch noninfectious EBOV VLPs as a second vaccine modality in the MVA-BN-EBOV-VLP-vaccinated organism. Human cells infected with either MVA-BN-EBOV-VLP or MVA-BN-EBOV-GP showed comparable GP expression levels and transport of complex N-glycosylated GP to the cell surface. Human cells infected with MVA-BN-EBOV-VLP produced large amounts of EBOV VLPs that were decorated with GP spikes but excluded the poxviral membrane protein B5, thus resembling authentic EBOV particles. The heterologous TAFV NP enhanced EBOV VP40-driven VLP formation with efficiency similar to that of the homologous EBOV NP in a transient-expression assay, and both NPs were incorporated into EBOV VLPs. EBOV GP-specific CD8 T cell responses were comparable between MVA-BN-EBOV-VLP- and MVA-BN-EBOV-GP-immunized mice. The levels of EBOV GP-specific neutralizing and binding antibodies, as well as GP-specific IgG1/IgG2a ratios induced by the two constructs, in mice were also similar, raising the question whether the quality rather than the quantity of the GP-specific antibody response might be altered by an EBOV VLP-generating MVA recombinant.

DOI: https://doi.org/10.1128/JVI.00343-17

Recombinant modified vaccinia virus Ankara generating Ebola virus-like particles

Marc Schweneker[1,*,#], Andrea S. Laimbacher[2,*], Gert Zimmer[3], Susanne Wagner[1], Elisabeth M. Schraner[4], Michael Wolferstätter[1], Marieken Klingenberg[1], Ulrike Dirmeier[1], Robin Steigerwald[1], Henning Lauterbach[1], Hubertus Hochrein[1], Paul Chaplin[1], Mark Suter[5], and Jürgen Hausmann[1,#]

[1] Bavarian Nordic GmbH, Fraunhoferstraße 13, D-82152 Martinsried, Germany; [2] Universität Zürich, Virologisches Institut, Winterthurerstrasse 266a, 8057 Zürich, Switzerland; [3] Institut für Virologie und Immunologie (IVI), Sensemattstrasse 293, 3147 Mittelhäusern, Switzerland; [4] Universität Zürich, Veterinär-Anatomisches und Virologisches Institut, Winterthurerstrasse 266a, 8057 Zürich, Switzerland; [5] Universität Zürich, Vetsuisse, Dekanat, Winterthurerstrasse 204a, 8057 Zürich, Switzerland.

*These authors contributed equally to this work.

Running title: MVA producing Ebola VLPs

Address correspondence to: Dr. Jürgen Hausmann, juergen.hausmann@bavarian-nordic.com, or Dr. Marc Schweneker, marc.schweneker@bavarian-nordic.com, Bavarian Nordic GmbH, Fraunhoferstraße 13, D-82152 Martinsried

Word count: abstract 234 words, text 7343 words

Abstract (234 words)

There are currently no approved therapeutics or vaccines to treat or protect against the severe hemorrhagic fever and death caused by Ebola virus (EBOV). Ebola virus-like particles (EBOV-VLPs) consisting of the matrix protein VP40, the glycoprotein (GP) and the nucleoprotein (NP) are highly immunogenic and protective in non-human primates against Ebola virus disease (EVD). We have constructed a modified vaccinia virus Ankara-Bavarian Nordic® (MVA-BN®) recombinant co-expressing VP40 and glycoprotein (GP) of EBOV Mayinga and the nucleoprotein (NP) of Taï Forest virus (TAFV) (MVA-BN-EBOV-VLP) to launch non-infectious EBOV-VLPs as a second vaccine modality in the MVA-BN-EBOV-VLP-vaccinated organism. Human cells infected with either MVA-BN-EBOV-VLP or MVA-BN-EBOV-GP showed comparable GP expression levels and transport of complex N-glycosylated GP to the cell surface. Human cells infected with MVA-BN-EBOV-VLP produced large amounts of EBOV-VLPs that were decorated with GP spikes but excluded the poxviral membrane protein B5, thus resembling authentic EBOV particles. The heterologous TAFV-NP enhanced EBOV-VP40-driven VLP formation with comparable efficiency as the homologous EBOV-NP in a transient expression assay, and both NPs were incorporated into EBOV-VLPs. EBOV-GP-specific CD8 T cell responses were comparably efficient between MVA-BN-EBOV-VLP and MVA-BN-EBOV-GP immunized mice. The levels of EBOV-GP-specific neutralizing and binding antibodies as well as GP-specific IgG1/IgG2a ratios induced by the two constructs in mice were also similar, raising the question whether the quality rather than the quantity of the GP-specific antibody response might be altered by an EBOV-VLP-generating MVA recombinant.

Importance (148 words)

The recent outbreak of Ebola virus (EBOV), claiming more than 11,000 lives, has underscored the need to advance the development of safe and effective filovirus vaccines. Virus-like particles (VLPs) as well as recombinant viral vectors have proved to be promising vaccine candidates. Modified vaccinia virus Ankara-Bavarian Nordic® (MVA-BN®) is a safe and immunogenic vaccine vector with a large capacity to accommodate multiple foreign genes. In this study, we combined the advantages of VLPs and the MVA platform by generating a recombinant MVA-BN-EBOV-VLP that would produce non-infectious EBOV-VLPs in the vaccinated individual. Our results show that human cells infected with MVA-BN-EBOV-VLP indeed formed and released EBOV-VLPs, thus producing a highly authentic viral immunogen. MVA-BN-EBOV-VLP efficiently induced EBOV-specific humoral and cellular immune responses in vaccinated mice. These results are the basis for future advancements, e.g. by including antigens from various filoviral species to develop multivalent VLP-producing MVA based filovirus vaccines.

Introduction

Most members of the family *Filoviridae* including ebolaviruses and marburgviruses cause severe hemorrhagic fevers with high fatality rates in humans and great apes (1,2). The genus *Ebolavirus* contains five virus species including *Zaire ebolavirus* and *Taï Forest ebolavirus*. The genomes of the members of these five species differ by more than 30% at the nucleotide level (3). Ebola virus (EBOV) is the type virus of the species *Zaire ebolavirus* and has been responsible for most of the known outbreaks of Ebola virus disease (EVD) in Africa. The case-fatality rate of this ebolavirus species ranges up to 90%, while only one human case of Taï Forest Virus (TAFV) infection has been reported so far that was non-fatal. However, TAFV infection can be lethal for cynomolgus macaques (4). The 2014/2015 epidemic of EVD in West Africa caused by a regional EBOV variant named Makona demonstrated that ebolaviruses not only give rise to locally restricted outbreaks but can also cause large and disastrous epidemics.

A total of 28 616 cases, including 11 310 deaths, have been counted during the recent West African Ebola epidemic (5). A number of vaccines against EVD are currently under development comprising virus-like particles (VLPs), an inactivated genetically modified EBOV, and various viral vectors, which include modified vaccinia virus Ankara-BN® (MVA-BN®), human and chimpanzee adenovirus, and vesicular stomatitis virus (VSV)(6-10).

EBOV-VLPs purified from the supernatant of cells expressing EBOV-GP, -VP40 and -NP have been demonstrated to protect non-human primates (NHP) against lethal challenge with the homologous EBOV (11). The EBOV matrix protein VP40 alone is able to drive the generation of filovirus-like particles with the typical filamentous morphology, but lacking the GP surface spikes of *bona fide* EBOV virions (12-15). Since EBOV-GP is the critical target antigen for the induction of protective immune responses (16,17), a minimal Ebola VLP vaccine should include GP and VP40. Moreover, GP enhances the efficacy of VP40-driven VLP formation, which can be further stimulated by co-expressing other EBOV proteins, in particular NP, but also VP30 and VP24 (18,19). Such EBOV-VLPs are non-infectious and thus safe since they lack viral genomic nucleic acid.

MVA-BN is a highly replication-restricted vaccinia virus derived from its replication-competent ancestor chorioallantois vaccinia virus Ankara by over 570 passages in chicken embryo cells (20). A large body of preclinical and clinical evidence is supporting the conclusion that MVA-BN is a safe and immunogenic vaccine, which has paved the way for the approval of MVA-BN (21) as a smallpox vaccine in the European Union and Canada. In addition, numerous MVA recombinants have been shown to efficiently induce immune responses in animals and humans against heterologous antigens (22,23). Recently, a recombinant MVA-BN expressing EBOV-GP together with other filovirus antigens was shown in human trials to efficiently enhance humoral and cellular responses directed to EBOV-GP, if used as prime or boost vaccination in combination with human or chimpanzee adenoviral vectors (7,9). This demonstrates the

potential of MVA-BN as a vaccine platform to protect against lethal hemorrhagic fevers of humans like EVD in combination with a heterologous viral vector.

To mimic the authentic structure of GP, the most relevant EVD vaccine antigen, as accurately as possible, we designed a recombinant MVA-BN vector vaccine generating EBOV-VLPs in the vaccinated organism. Such VLPs would provide a second vaccine modality in the vaccinated individual in addition to the vector-driven cell-restricted expression of EBOV proteins. Here, we describe a recombinant MVA-BN (MVA-BN-EBOV-VLP) that was engineered to express EBOV-VP40 along with EBOV-GP and TAFV-NP in infected cells. The TAFV version of NP was chosen to provide for a broader representation of T cell antigens from different ebolavirus species in the vaccine construct. This recombinant virus directed the release of EBOV-VLPs that were densely decorated with EBOV-GP on their surface into the supernatant of infected cells, demonstrating that EBOV-VLP morphogenesis was compatible with the MVA platform. NP from EBOV and TAFV both enhanced the formation of VLPs driven by EBOV-VP40 and were found in VLPs. MVA-BN-EBOV-VLPs efficiently induced GP-specific cellular and humoral immune responses in mice, which were quantitatively comparable to those induced by MVA-BN-EBOV-GP expressing only GP.

Materials and Methods

Cells, viruses and antibodies

The human cervical carcinoma HeLa (CCL-2), human embryonic kidney HEK 293T/17 (CRL-11268) and baby hamster kidney BHK-21 (CCL-10) cell lines cells were obtained from ATCC, Vero E6 cells were obtained from the European Cell Culture Collection via Sigma (cat no. 85020206). All cell lines were cultivated in Dulbecco's modified Eagle medium (DMEM, Gibco/Invitrogen, Darmstadt, Germany) supplemented with 10% fetal calf serum (FCS, Pan Biotech, Aidenbach, Germany). Primary chicken embryo fibroblast (CEF) cells were prepared from 11 day-old embryonated chicken eggs and cultured in VP-SFM (Gibco) for virus stock

production or in RPMI supplemented with 7% FCS for titration assays. The MVA used in this study was either MVA-BN® (Bavarian Nordic GmbH, Munich) or an MVA wild-type (wt), which was derived from a bacterial artificial chromosome (BAC) clone constructed from MVA-BN. The properties of the latter, containing a BAC cassette including an NPT II-IRES-enhanced green fluorescent protein (EGFP) array of selectable markers, were indistinguishable from those of MVA-BN (24). MVA-BN, MVA-BN recombinants and MVA wt were propagated on primary or secondary CEF cells and titrated on secondary CEF cells using the $TCID_{50}$ method as described (25). The murine monoclonal antibodies 6D8 against EBOV GP and 9G4 against Marburg virus (MARV)-Musoke GP were obtained from J. Biggins (US Army Medical Research Institute of Infectious Diseases, Fort Detrick, MD, USA). The anti-TAFV-NP antibody was generated for Bavarian Nordic by BioGenes GmbH, Berlin, Germany, against a TAFV-NP-derived peptide with the sequence CVSGSENTDNKPHSE. Rabbit polyclonal anti-EBOV-NP (#0301-012) and anti-EBOV-VP40 (#0301-010) antibodies were obtained from IBT Bioservices, Gaithersburg, MD, USA. The rabbit polyclonal B5-specific antibody was a gift from Dr. Robert Drillien, I.G.B.M.C., 67400 Illkirch-Graffenstaden, France.

Generation of recombinant viruses

MVA-BN-EBOV-GP and MVA-BN-EBOV-VLP recombinants were generated using transient dominant selection (26) according to standard procedures. The cDNAs encoding VP40 and GP of *Zaire ebolavirus* variant Mayinga and NP of *Taï Forest ebolavirus* (TAFV) were synthesized by Invitrogen GeneArt (Regensburg, Germany). The recombinant viruses still contained the NPT II/RFP cassette (MVA-BN-EBOV-GP) or both cassettes (MVA-BN-EBOV-VLP). Recombinant EBOV-VP40 and TAFV-NP expression was driven by the PrS promoter (27) while the EBOV-GP gene was under control of the PrS5E promoter containing five additional tandem repeats of the p7.5k promoter (28) in both MVA recombinants. A recombinant chimeric VSV (VSV-EBOV-GP) was generated by replacing the VSV G gene with the EBOV-GP gene (variant

Mayinga) according to published procedures (29). VSV-EBOV-GP also expressed EGFP from an additional transcription cassette downstream of the GP gene. In addition, VSV-EBOV-GP encoded for a modified VSV-M gene containing 4 point mutations (M_Q) known to reduce cytotoxicity of the virus and to induce type I IFN in IFN-competent cells (30). VSV-EBOV-GP was propagated and titrated on Vero and BHK-21 cells.

Transient transfections

cDNAs optimized for human codon usage encoding EBOV-VP40, EBOV-NP and TAFV-NP were synthesized by GeneArt (Regensburg, Germany) and subcloned into MVA recombination plasmids (Bavarian Nordic, Munich, Germany) under the control of the synthetic PrS vaccinia virus promoter. For cellular expression, subconfluent cells in 12-well tissue culture plates were infected with MVA-BN® at a multiplicity of infection (MOI) of 5. At 1 h post infection (p.i.), cells were transfected with FuGene® HD/6 (Promega, Mannheim, Germany) according to manufacturer's instructions, using a total of 3 µg plasmid DNA and 9 µl of transfection reagent per well.

Glycosylation analysis

Infected cells were lysed in RIPA buffer (New England Biolabs, Frankfurt, Germany), cell lysates divided into three aliquots and treated with either Endo H or PNGase F (New England Biolabs, Frankfurt, Germany) according to manufacturer's instructions or mock treated. For Western blot analysis, samples were mixed with 3x Laemmli sample loading buffer.

Immunoblot analysis EBOV and TAFV proteins

HeLa and HEK 293T/17 cells were seeded on the day before infection. Inoculation, cell lysate preparation, immunoblotting, immunodetection and stripping were performed as previously described (31). For SDS-PAGE, 7.5% Mini-Protean TGX polyacrylamide gels were used (Bio-

Rad, Munich, Germany). Antibodies used for immunodetection were diluted as follows: anti-EBOV-GP mAb 6D8, anti-EBOV-VP40 and anti-EBOV-NP 1:1000, anti-TAFV-NP 1:10,000. Detection of protein bands by enhanced chemiluminescence (ECL) was carried out with two alternative substrate reagents depending on signal strength, SuperSignal West Pico (Thermo Scientific, Bonn, Germany) as the standard reagent and ECL Advance Western Blotting Detection Kit (GE Healthcare, Munich, Germany) for detection with higher sensitivity. Western blot images were acquired using Kodak BioMax Light Films (Sigma-Aldrich, Munich, Germany) or the ChemiDoc Touch System and Image Lab™ Software (Bio-Rad, Munich, Germany) for image analysis and quantification.

Reverse transcriptase quantitative real-time PCR

Infection/transfection controls for RT-qPCR were set up in triplicate per condition and RNA from 1-1.5x10^6 infected HEK293T/17 cells per sample was isolated as previously described (32). Reverse transcription of 3 µl of isolated RNA was performed using the Omniscript RT kit (205113, Qiagen) in the presence of an RNase inhibitor (R2520, Sigma-Aldrich) at a final concentration of 10 U/µl for 70 min at 37°C using random nonamer primers at a final concentration of 5 µM (R7647, Sigma-Aldrich). 1 µl of RT reaction was added to 20 µl of total PCR reaction mixture for quantitative real-time PCR based on the TaqMan® Gene Expression Master Mix (4369016, Life Technologies, Darmstadt, Germany) according to the manufacturer's instructions. Quantitative PCR of cDNA was performed using the following primers and TaqMan® probes: EBOV-NP fw primer: GCAGTCTGTCGGGCATATGA (final conc. 500 nM), EBOV-NP rev primer: CTTTCAGTCTTTTGGAGGATGTG (final conc. 500 nM), EBOV-NP probe: FAM-TCAAGGCATGCATATGGTCGCC- MGBNFQ (final conc. 252 nM), TAFV-NP fw primer: GAGCGTGGGCCACATGA (final conc. 500 nM), TAFV-NP rev primer: TCGGTTTTCTGCAGGATGTG (final conc. 500 nM), TAFV-NP probe: FAM-CCAGGGAATGCACATGGTGGCT- MGBNFQ (final conc. 252 nM). The EBOV-NP- and TAFV-

NP-specific primer/probe sets were used as a 1:1 mix in a multiplex qPCR reaction. Input cDNA was normalized using TaqMan® gene expression assay 18S (Hs99999901_s1) detecting eukaryotic 18S rRNA transcripts. All real-time qPCR reactions were performed in duplicate using an Applied Biosystems 7500 Real-Time PCR System with initial incubation at 50°C for 2 min (uracil DNA glycosylase activation), 10 min incubation at 95°C, and 40 cycles of 15 s at 95°C and 1 min at 60°C. No-template controls and minus-RT controls were uniformly negative. Fold transcription of NP was calculated relative to cells not expressing NP. Ct values were arbitrarily set to 36 if Ct value was “undetermined” or > 36.

Flow cytometry

Infected and uninfected cell monolayers were washed with PBS and single cell suspensions were prepared by scraping and thoroughly resuspending the cells. Cells were washed and resupended in ice-cold PBS containing 2% FCS, stained using anti-EBOV-GP monoclonal antibody 6D8 (1:2500) followed by staining with an allophycocyanin-coupled anti-mouse secondary antibody (1:1000). Cells were analyzed for GP surface expression, as well as cytoplasmic EGFP and RFP expression by flow cytometry using a LSR II flow cytometer (BD Biosciences, Heidelberg, Germany) and FlowJo software (Tree Star Inc., Ashland, OR, USA).

Preparation of EBOV-VLPs

EBOV-VLPs in supernatants of MVA-BN-EBOV-VLP infected cells were concentrated and purified by centrifugation through a 20% sucrose cushion at 36,000 rpm in a Beckmann SW41 rotor for 2 h. The pellet was thoroughly resuspended in ice-cold PBS containing protease inhibitor cocktail (Roche cOmplete; Sigma-Aldrich, Munich, Germany), by initial vortexing and then rotating the samples for 1 h at 4°C.

Confocal immunofluorescence analysis of recombinant EBOV protein expression

HeLa cells were grown on 12 mm coverslips (0.17 mm thick), infected at a MOI of 10 with the recombinant MVA vectors and fixed 6 h p.i. with 3.7% formaldehyde in PBS. After permeabilization with PBS containing 0.1% Triton X-100, the cells were blocked with PBS supplemented with 3% bovine serum albumin (PBS-BSA). Cells were incubated with the corresponding antibodies diluted in PBS-BSA: murine monoclonal antibody 6D8 against EBOV-GP 1:200, rabbit polyclonal anti-TAFV-NP antibody 1:500, rabbit polyclonal anti-EBOV-VP40 1:250. As secondary antibodies, goat anti-rabbit IgG (H+L)-Alexa Fluor 405 or goat anti-mouse IgG(H+L)-Alexa Fluor 633 (Molecular Probes, Invitrogen, USA) were used at a dilution of 1:500. After washing with PBS and H_2O, the coverslips were mounted in Prolong Gold (Molecular Probes, Invitrogen, USA). Samples were analyzed using a confocal laser-scanning microscope SP8 (Leica Microsystems, Wetzlar, Germany, 63x oil objective).

Immunoelectron microscopy

For immunoelectron microscopy (immuno-EM), samples were adsorbed to carbon-coated parlodion films mounted on 300 mesh/inch copper grids (EMS, Fort Washington, PA, USA) for 10 min, blocked with PBS containing 0.1% BSA (PBS-BSA/0.1%) for 10 min, incubated with the primary antibody diluted in PBS-BSA/0.1% (murine monoclonal antibody 6D8 against EBOV-GP 1:50, murine monoclonal antibody 9G4 against MARV-GP 1:50, rabbit polyclonal anti-B5 1:400) for 1 hour, washed several times with PBS-BSA/0.1%, incubated with the secondary anti-IgG antibody coupled to 12 or 18 nm colloidal gold particles (Jackson ImmunoResearch, West Grove, PA, USA) diluted 1:15 (18 nm) or 1:30 (12 nm) in PBS-BSA/0.1%, washed several times with PBS and H_2O and stained with 2% phosphotungstic acid (PTA), pH 7.0 (Aldrich, Steinheim, Germany) for 1 min. Specimens were analyzed in a transmission electron microscope (CM12, Philips, Eindhoven, Netherlands) equipped with a CCD camera (Ultrascan 1000, Gatan, Pleasanton, CA, USA) at an acceleration voltage of 100 kV.

Preparation and analysis of ultrathin sections

HeLa cells either grown on sapphire disk or in 6-well tissue culture plates were infected at a MOI of 10 with the recombinant MVA vectors. After 12-24 h, the cells were either scraped into the medium and the cell pellet was fixed in 2.5% glutaraldehyde (GA) by centrifugation for 20 min at 4000 g, or the sapphire disks were fixed in 2.5% GA for 1 hour at 4 °C before embedding in epon according to a standard protocol (33). Briefly, after fixation with 2.5% GA, cells were postfixed with 1% osmium tetroxide (OsO_4), dehydrated in a graded ethanol series starting at 70% and, after two changes in acetone, embedded in epon. Ultrathin sections were stained with uranyl acetate and lead citrate and were analyzed in a transmission electron microscope as described above. (CM12, Philips, Eindhoven, Netherlands) equipped with a CCD camera (Ultrascan 1000, Gatan, Pleasanton, CA, USA) at an acceleration voltage of 100 kV.

Enzyme-linked immunosorbent assay (ELISA) and plaque reduction neutralization test 50 (PRNT50)

For immunization 6-8 week-old CBA mice (Janvier Labs, Le Genest Saint Isle, France) were used (group size n=5). The animals were immunized intramuscularly into the hind leg with 10^8 $TCID_{50}$ of either MVA-BN-EBOV-GP or MVA-BN-EBOV-VLP in 50 µl sterile PBS on days 0 and 28. Blood samples were taken on days 21, 42 and 56 and serum was prepared to determine Ebola virus GP-specific IgGs by direct ELISA. 96-well plates were coated overnight with recombinant EBOV-GP antigen (total IgG, 0.625 µg/ml; IgG1, 0.64 µg/ml; IgG2a 0.32 µg/ml) (IBT Bioservices, Rockville, MD, USA). Test sera were titrated in duplicate using twofold serial dilutions. The plates were incubated for 1 h at room temperature, washed and incubated for 1 h with detection antibody sheep or goat anti-mouse IgG-HRP, IgG1-HRP or IgG2a-HRP (1:2,000 dilution) (Bio-Rad, Munich, Germany). Plates were washed and developed using 3.3′5.5′-tetramethylbenzidine at room temperature in the dark, the reaction was stopped after 30 min

(total IgG) or 15 min (IgG1/2a) using H_2SO_4 and read out at 450 nm (TECAN Sunrise ELISA plate reader).

For PRNT50, a chimeric VSV construct in which the authentic G spike glycoprotein was replaced by EBOV-GP was used to determine the titer of EBOV-neutralizing antibodies in sera of immunized mice. Serial dilutions of mouse antiserum were incubated in duplicate with ~100-150 pfu of VSV-EBOV-GP per dilution and plated on Vero cells for three days. The monolayers were stained with crystal violet and scanned with a flat bed scanner. The electronic images of the monolayers were then analyzed by neuronal network software (NN plate count, developed in-house) recognizing and counting the plaques and calculating the PRNT50.

Results were analyzed by an unpaired two-tailed Student´s t test. p-values of < 0.05 were considered statistically significant.

EBOV-GP-specific CD8 T cell response

CBA mice were immunized by intramuscular (i.m.) or intravenous (i.v.) application of 10^8 $TCID_{50}$ of MVA-BN-EBOV-GP or MVA-BN-EBOV-VLP on days 0 and 28 (group size n=5). The CD8 T cell response against the immunodominant GP epitope in the H-2k haplotype (TELRTFSI) was determined by dextramer staining of peripheral blood mononuclear cells on days 8 and 5 after prime and boost, respectively. For intracellular cytokine staining, immunized mice were sacrificed at d56 (28 days after the last immunization), spleens were harvested on ice and mononuclear spleen cell suspensions were prepared. Cells were incubated with 5 µg/ml of MHC class I restricted EBOV-GP-derived peptide (TELRTFSI) (GenScript, Piscataway, NJ, USA) for 5–6 h at 37°C in complete RPMI in the presence of 1 µl/ml GolgiPlug (BD Biosciences, Heidelberg, Germany), and anti-CD107 (FITC) (BioLegend, San Diego, CA, USA). Cell surface marker expression was analyzed with anti-CD4 (BV650), anti-CD8 (BV785) (both BioLegend) and anti-CD44 (APC-eFluor780) (eBiosciences, San Diego, CA, USA) antibodies. For live/dead cell discrimination, cells were stained with LIVE/DEAD fixable aqua dead cell staining kit

according to the manufacturer's instructions (Life Technologies GmbH, Darmstadt, Germany). Intracellular cytokine staining of IFN-γ (PE-Cy7), TNF-α (PerCP-eFluor710) and IL-2 (APC) (all eBiosciences) was performed after fixation and permeabilization according to the manufacturer's instructions (BD Cytofix/Cytoperm, BD Biosciences). Flow cytometric analysis was performed using a digital LSR II (BD Biosciences). Data were analyzed with FlowJo software (Tree Star Inc., Ashland, OR, USA). Results were analyzed by an unpaired two-tailed Student´s t test. p-values of < 0.05 were considered statistically significant.

Results

Recombinant MVA constructs MVA-BN-EBOV-GP and MVA-BN-EBOV-VLP

The aim of this study was to generate a recombinant MVA-BN vector to protect against EVD that not only expresses the major protective antigen GP but that also triggers the production of EBOV-VLPs in infected cells. For this, the genes encoding VP40 and GP, both derived from the Mayinga variant of EBOV, and NP derived from TAFV were inserted into intergenic regions (IGRs) of MVA-BN® under the control of the early/late vaccinia virus promoters PrS and PrS5E (Fig. 1A). PrS5E contains the PrS compact synthetic early/late promoter and five additional Pr7.5 early elements (27,28).

Expression of EBOV-GP was studied by Western blot analysis of cell lysates from HeLa cells infected with MVA-BN-EBOV-GP or MVA-BN-EBOV-VLP. Two distinct bands were observed in lysates of cells infected with either MVA-BN-EBOV-GP or MVA-BN-EBOV-VLP (Fig. 1B). The upper band detected at 6 h and 24 h p.i. (Fig. 1B, lanes 3 to 6) likely represents the mature, fully N- and O-glycosylated GP which has been proteolytically cleaved into the large subunit GP_1 and the small subunit GP_2. GP_2 was not recognized by the antibody used. In addition, the mature GP_1 could not be distinguished from the uncleaved and fully glycosylated precursor GP (preGP) due to the very similar migration of these two forms in our SDS-PAGE system. The lower band

(Fig. 1B, lanes 3, 5) was detected at 6 h but not at 24 h p.i. and presumably represents the immature and unprocessed GP precursor protein residing in the endoplasmic reticulum (pre-GP_{ER}) (34,35). GP_1 and the uncleaved precursor preGP have a larger apparent molecular weight than $preGP_{ER}$ due to extensive O-glycosylation and maturation of the N-glycans from the high-mannose to the complex-type form (35,36). Lysates of cells infected with MVA-BN-EBOV-GP or MVA-BN-EBOV-VLP revealed a very similar pattern of EBOV-GP-specific bands indicating similar GP processing and maturation (Fig. 1B).

To further characterize the two major forms of recombinant EBOV-GP, we analyzed N-glycosylation of the protein by using two different endoglycosidases. Endoglycosidase H (Endo H) removes N-glycans of the high-mannose type which have been co-translationally attached to the protein in the ER. During transport of glycoproteins through the Golgi apparatus, their N-glycans are further processed to the complex type, rendering them resistant to Endo H. Both, ER- and Golgi-resident N-glycans are sensitive to PNGase F, which removes high-mannose, hybrid, as well as complex N-glycans. However, O-linked glycans, which are added to EBOV-GP in the Golgi apparatus, are not susceptible to either of the two enzymes. HeLa cell lysates prepared 17 h p.i. with MVA-BN-EBOV-GP or MVA-BN-EBOV-VLP were either mock-treated or incubated with Endo H or PNGase F and analyzed by immunoblot (Fig. 1C). The upper band, likely representing GP_1/preGP, turned out to be resistant to Endo H-mediated deglycosylation, indicating that this GP form had left the ER and entered the Golgi apparatus. In contrast, the faster migrating band, presumably representing uncleaved $preGP_{ER}$ (35,36) was clearly affected by Endo H digestion, indicating that a proportion of EBOV-GP still resided in the ER late in infection (Fig. 1C, lanes 2 and 5). We were not able to distinguish between GP_1 and Endo H-resistant preGP in our gel system. Treatment with PNGase F affected the migration of both the upper and the lower EBOV-GP band and generated an additional GP species that migrated in the gel as a broad and prominent smear (Fig. 1C, lanes 3 and 6), likely representing the de-N-glycosylated but still O-glycosylated EBOV-GP.

Flow cytometric analysis of HeLa cells infected with either MVA-BN-EBOV-GP or MVA-BN-EBOV-VLP showed that EBOV-GP was already present at the cell surface in large amounts at 4 h p.i. (Fig. 1D). EBOV-GP levels were only slightly increased when the cells were analyzed 24 h p.i. No significant differences in EBOV-GP cell surface expression levels were detected between cells infected with MVA-BN-EBOV-GP and MVA-BN-EBOV-VLP.

In addition to expression of GP, HEK 293T/17 cells infected with MVA-BN-EBOV-VLP also expressed EBOV-VP40 and TAFV-NP as indicated by detection of specific bands in immunoblots at approximately 40 kDa and 100 kDa, respectively (Fig. 1E). In summary, no obvious differences in intracellular and cell surface expression levels and glycosylation of EBOV-GP were observed throughout the time course of infection with MVA-BN-EBOV-GP and MVA-BN-EBOV-VLP (Fig. 1B-D). These results indicate that neither any MVA-BN factors nor co-expression of VP40 and NP interfered with the transport or N-glycosylation of EBOV-GP along the secretory pathway.

Intracellular distribution of Ebola proteins in MVA-BN-EBOV-VLP infected cells

Confocal laser-scanning microscopy was used to examine the synthesis and subcellular localization of EBOV-GP, EBOV-VP40 and TAFV-NP with specific antibodies (Fig. 2). EGFP fluorescence (selection marker in MVA-BN-EBOV-VLP or MVA wt, shown in grey) and RFP fluorescence (selection marker in MVA-BN-EBOV-VLP or MVA-BN-EBOV-GP, shown in grey) were used to identify vector infected cells. In both, cells infected with MVA-BN-EBOV-VLP or MVA-BN-EBOV-GP infected cells, EBOV-GP was mainly located at the cell membrane where it was present in long cellular protrusions (Fig. 2, first two panels, in green). Similar to EBOV-GP, the matrix protein EBOV-VP40 was strongly associated with the cell membrane (Fig. 2, middle two panels, in magenta). TAFV-NP formed large aggregates in the cytoplasm that resembled typical inclusion bodies (Fig. 2, last two panels, in cyan). In addition to these large NP aggregates, there were smaller aggregations of TAFV-NP that were closely associated with the

plasma membrane (Fig. 2, upper right panels). Since VP40 is also located mainly at or below the plasma (Fig. 2, upper middle panels) it is very likely that a fraction of VP40 and NP colocalized, though this could not formally be proven due to technical constraints. Taken together, the subcellular localization of the MVA encoded ebolavirus proteins was consistent with previously published data (37) and further supports and extends our initial observation by confirming that MVA infection does not interfere with the intracellular distribution of GP, VP40 and NP.

Ebola VLPs in supernatants of MVA-BN-EBOV-VLP infected cells

We prepared VLPs from supernatants of cells infected with MVA-BN-EBOV-VLP and analyzed these preparations as well as plain supernatants and cellular lysates for the presence of EBOV-GP, EBOV-VP40 and TAFV-NP. Infections with MVA-BN-EBOV-GP and MVA-BN wt were included as controls (Fig. 3). Levels of GP were slightly higher in lysates of cells infected with MVA-BN-EBOV-GP when compared to MVA-BN-EBOV-VLP. EBOV-GP was detectable in supernatants and in sucrose cushion-purified supernatants from MVA-BN-EBOV-GP infected cells, indicative of GP release in form of pleomorphic particles as described previously (15,36). In comparison, GP levels were higher in the supernatants and VLP preparations from cells infected with MVA-BN-EBOV-VLP (Fig. 3). Thus, more GP was released upon co-expression of VP40 and TAFV-NP, most likely by formation of EBOV-VLPs. VP40 was also present in supernatants and was highly enriched in VLP preparations, indicating the formation of VP40-driven VLPs by MVA-BN-EBOV-VLP infected cells (Fig. 3). The smaller VP40 forms most likely represent a translation product initiated at the internal methionine residue 14 and degradation products as previously described (38). TAFV-NP was also detectable in VLP preparations but not in plain supernatants, implying that TAFV-NP had been incorporated in a species independent manner into VLPs driven by EBOV-VP40 expression.

To obtain detailed visual information on MVA-driven EBOV-VLP formation, ultrathin sections of infected HeLa cells were analyzed by transmission electron microscopy (TEM). At 24 h p.i. with MVA-BN-EBOV-VLP, several longitudinal as well as cross sections through filamentous structures were detected which resembled typical EBOV virions at the stage of budding from the plasma membrane (Fig. 4A). These virus-like structures differed from cellular filopodia by their consistently smaller diameter. Cellular filopodia were also present in MVA infected control cells (Fig. 4B). Concentrated, purified VLP preparations from the supernatant of MVA-BN-EBOV-VLP infected cells revealed the release of filamentous particles typical for EBOV-VLPs (Fig. 4C). Immuno-EM labeling with an EBOV-GP-specific monoclonal antibody resulted in the decoration of the surface of the filamentous particles with gold beads specifically identifying these particles as EBOV-VLPs (Fig. 4C). No labeling of the filamentous particles was detectable using a MARV-GP-specific antibody (data not shown), confirming specificity of the labeling reaction. The concentrated supernatant of MVA-BN-EBOV-GP infected cells contained some pleomorphic particles that were also labeled by the EBOV-GP-specific antibody (Fig. 4D). Such non-filamentous EBOV-GP positive particles were also present in the supernatant of MVA-BN-EBOV-VLP infected cells (Fig. 4C, bottom left) and were most likely the result of a GP-dependent but VP40-independent budding process (15,36). In preparations of supernatant from MVA-BN infected cells, no GP positive particles were detected (Fig. 4E). These findings indicate that the filamentous particle shown in Fig. 4C represents a *bona fide* Ebola VLP which was released from MVA-BN-EBOV-VLP infected cells.

Vaccinia virus protein B5 is excluded form EBOV-VLP

Vaccinia virus encoded proteins of the outer membrane of the extracellular vaccinia virus (EV) including the B5 protein have been shown to partly localize to the plasma membrane of infected cells (39). We therefore analyzed whether the B5 protein, an important component of the poxviral EV membrane, would also be incorporated into EBOV-VLPs. Double immunogold-

labeling and TEM analysis of concentrated VLP preparations from MVA-BN-EBOV-VLP infected cells revealed that the B5 protein (18 nm gold particles) was exclusively localized in non-viral particulate structures that did not overlap with EBOV-GP positive particles (12 nm gold particles, Fig. 4F), suggesting that this MVA protein is excluded from VLPs. This also applied to the pleomorphic particles released from MVA-BN-EBOV-GP infected cells (Fig. 4G). After infection with MVA-BN, particulate structures were only stained by the 18 nm gold particle-conjugated antibody directed to B5 protein, but not with antibodies specifically recognizing the EBOV-GP (Fig. 4H). Most likely, the B5 protein positive structures represent membranous vesicles that were derived from cellular compartments like the Golgi apparatus, the *trans*-Golgi network, endosomes or the plasma membrane. These data confirm previous observations showing that the formation of ebolavirus-like particles at the plasma membrane is a specific process that excludes other proteins from incorporation into the VLPs (13,40,41).

Incorporation of NP into EBOV-VLPs

EBOV-NP is incorporated into VLPs formed by expression of homologous EBOV-VP40 (42,43). Although TAFV-NP was expressed along with EBOV-GP and EBOV-VP40 by HEK 293T/17 cells infected with MVA-BN-EBOV-VLP (Fig. 1E, 3), cross-sections of EBOV-VLPs appeared to be “empty” (Fig. 4A), suggesting that the EBOV-VLPs produced by MVA-BN-EBOV-VLP did not contain nucleocapsid-like structures. In order to analyze whether TAFV-NP is incorporated into EBOV-VP40-derived VLPs and whether it can enhance VLP formation in a species-independent fashion, a VLP formation assay based on plasmid-based EBOV-NP and TAFV-NP expression in MVA infected cells was used. Plasmids encoding either TAFV-NP or EBOV-NP under the control of the vaccinia virus early-late promoter PrS were transfected into MVA infected HEK 293T/17 cells along with a plasmid encoding EBOV-VP40 under the control of the same promoter.

Western blot analysis of the cell lysates demonstrated that VP40 levels were not grossly affected by co-expression of either EBOV-NP or TAFV-NP (Fig. 5A, top panel). To analyze whether NP and VP40 were released into the supernatant of transfected cells as part of VLPs, we removed soluble VP40 dimers and soluble NP by ultrafiltration through an Amicon® Ultra 100 kDa cut-off filter. Analysis of such purified and concentrated supernatants showed that the amount of VLP-associated VP40 in purified supernatants was 3.2-fold enhanced by co-expression of EBOV-NP. TAFV-NP enhanced VLP release by 2.7-fold, suggesting that both NPs did not significantly differ in this aspect (Fig. 5A, top panel). Compared to NP levels found in cell lysates, the proportion of VLP-associated NP in purified supernatants was also similar for both EBOV-NP (1/18) (Fig. 5A, middle panel) and TAFV-NP (1/21) (Fig. 5A, bottom panel). Because two different NP-specific antibodies had to be used for Western blot analysis of EBOV-NP and TAFV-NP, expression levels of the NPs could not be directly compared. To provide indication for equal expression levels of both NPs, we confirmed that EGFP, which is co-expressed from the NP-encoding plasmids, was present at similar levels (data not shown). In addition, TaqMan® RT-qPCR indicated that transcript levels of EBOV-NP and TAFV-NP were very similar (data not shown). Thus, the capacity of both TAFV-NP and EBOV-NP to enhance EBOV-VLP formation appeared to be very similar.

The presence of B5 in non-viral particulate structures of EBOV-VLP preparations and in purified supernatants of MVA infected cells not generating EBOV-VLPs (Fig. 4F-H) was also confirmed by Western blot. Expression of filovirus proteins EBOV-VP40, EBOV-NP or TAFV-NP in MVA-BN infected cells did not affect the release of B5 into supernatants (Fig. 5B) while VP40 release was enhanced by NP (Fig. 5A). This result supports the notion that B5 was not incorporated into VP40-driven EBOV-VLPs but was rather secreted by a different and spatially separated mechanism. Likely, B5 was contained in exosome-like vesicles that have previously been reported to be released from MVA infected cells (44).

Detection of nucleocapsid-like structures in MVA-driven EBOV-VLPs

Co-expression of NP with VP40 results in formation of a nucleocapsid-like structure visible as an inner ring in electron micrographs of VLP cross-sections (43), termed “bull´s eye” by Johnson et al. (43). We were unable to discern nucleocapsid-like structures in cross-sections of VLPs produced by cell infected with MVA-BN-EBOV-VLP (Fig. 4A and data not shown) although TAFV-NP was detected in VLPs as indicated by Western blot analysis (Fig. 3). Using the transfection approach described above, we compared the morphology of VLPs in ultrathin sections of HeLa cells expressing EBOV-VP40 along with either EBOV-NP or TAFV-NP. Cross-sections of VLPs generated in the presence of EBOV-NP clearly revealed nucleocapsid-like ring structures (Fig. 6A), indicating that EBOV-NP has been incorporated into VLPs. In contrast, most VLPs generated in the presence of TAFV-NP either appeared empty (Fig. 6B, 4A) or were filled with an amorphous structure or sometimes with an irregular-shaped, but not ring-like structure (data not shown). When 18 cross sections through VLPs released from VP40 and EBOV-NP expressing cells were analyzed, 9 had a clear inner ring, 8 showed a central irregular-shaped structure and one was empty. In contrast, of 77 cross-sections of EBOV-VLPs, which were generated in the presence of TAFV-NP (either by MVA-BN-EBOV-VLP infection or by VP40/TAFV-NP plasmid-based co-expression), 65 were empty, 11 had some internal irregular structure and only two showed a ring-like structure.

We conclude from these findings that the incorporation of NP into EBOV-VLPs and the enhancement of release of EBOV-VP40 VLPs occurs species-independent in the *Ebolavirus* genus (Fig. 3, 5A). The results from our EM analyses suggest, however, that the characteristic inner ring structure is efficiently formed only if the homologous EBOV-NP is present.

Induction of GP-binding and neutralizing antibodies by MVA-BN-EBOV-VLP in mice

Since EBOV-GP-specific antibody responses are considered most important for assessing the protective potential of EBOV vaccine candidates (16,17), we compared the induction of EBOV-

GP-specific antibodies in CBA mice following immunization with MVA-BN-EBOV-VLP and MVA-BN-EBOV-GP. Mice were vaccinated intramuscularly on days 0 and 28 and binding as well as neutralizing antibody responses on days 21, 42, and 56 were analyzed by ELISA and by PRNT using chimeric VSV-EBOV-GP as surrogate virus. Binding or neutralizing antibody titers of the immune sera from the two mouse groups did not significantly differ at any time point after priming or boosting (Fig. 7A, B and data not shown). To evaluate one qualitative aspect of the antibody response, we analyzed the levels of EBOV-GP-specific isotypes IgG1 and IgG2a. Although there appeared to be a tendency towards lower IgG1 and higher IgG2a levels of MVA-BN-EBOV-VLP-induced GP-specific antibodies compared to the respective IgG1 and IgG2a titers induced by MVA-BN-EBOV-GP (Fig. 7C, D), all of these differences where not statistically significant and the tendency was undetectable in a second independent mouse experiment. These results suggest that in this animal model, with the route and vaccine dose used, EBOV-VLP formation by a recombinant MVA vector did not significantly enhance the induction of EBOV-GP-specific antibodies or alter the IgG1/IgG2a isotype ratio compared to MVA-driven expression of EBOV-GP alone.

GP-specific CD8 T cell response

The EBOV-GP-specific CD8 T cell response following a prime-boost immunization regimen was analyzed in CBA/J mice, since the GP-derived CD8 T cell epitope inducing the strongest responses has been reported to occur in the H-2k haplotype. Shown is the GP-specific memory CD8 T cell response determined by intracellular staining of splenocytes for the cytokines IFN-γ, TNF-α and IL-2 as well as by surface staining of the degranulation marker CD107a at day 28 after the last immunization. There was a moderately lower frequency of GP-specific CD8 T cells in the spleens of MVA-BN-EBOV-VLP immunized mice compared to MVA-BN-EBOV-GP. This moderate difference was statistically significant between the two groups immunized by the i.v.

route for most of the markers except IL-2 (Fig. 8), but not in mice immunized by the i.m. route. In contrast, the geometric mean fluorescence intensity of the signal for intracellular IFN-γ and TNF-α was slightly higher in CD8 T cells of MVA-BN-EBOV-VLP immunized mice independent of the immunization route (Fig. 8). This difference was again statistically significant between the two i.v. immunized groups. Average total numbers of GP-specific CD8 T cells in the spleens of the two groups were similar (data not shown) reflecting the frequency results shown in Fig. 8. Frequencies of GP-specific CD8 T cells in blood on days 8 and 5 after prime and boost, respectively, determined by dextramer staining were also very similar between both groups independent of the immunization route (data not shown). In conclusion, the GP-specific CD8 T cell response induced by MVA-BN-EBOV-VLP was comparable to that induced by MVA-BN-EBOV-GP. The slightly lower frequency of GP-specific T cells in the spleen induced by MVA-BN-EBOV-VLP might be explained by the strong expression of the two additional potential CD8 T cell targets, VP40 and NP.

Discussion

VLPs represent a vaccine modality with excellent immunogenicity and efficacy, as demonstrated by successful vaccination programs employing approved VLP-based vaccines for protection against hepatitis B and human papilloma virus-induced cervical cancer (45). With respect to filoviruses, EBOV-VLPs and MARV-VLPs have been shown to provide protection from EVD and MVD, respectively, in a number of animal models including the non-human primate (NHP) model (11,46-49), which represents the best available animal model for human EVD. Protection of NHPs was initially achieved with a three-dose immunization regimen and involved use of adjuvants (11,46). A follow-up study showed that two immunizations with adjuvanted ebolavirus VLPs are already sufficient to protect NHPs from EBOV challenge (49). In the present study, we generated and characterized a novel MVA-BN-based vaccine vector which simultaneously

expressed three ebolavirus proteins driving the formation of ebolavirus-like particles in vector infected cells.

There is evidence from published literature showing that MVA might interfere with efficient transport of MARV-GP along the secretory pathway in human cells (50). Since budding of EBOV-VLPs takes place at the plasma membrane, such deficiency in transport competence might result in VLPs lacking GP. However, EBOV-GP expressed by MVA, either alone or in combination with VP40 and NP, was properly processed and transported to the cell surface, providing authentic GP antigen for VLP incorporation. In fact, the MVA-driven EBOV-VLPs were found to be decorated with GP spikes at high density (Fig. 4C, F), indicating that MVA did not interfere with incorporation of the viral glycoprotein into VLPs.

Foreign envelope glycoproteins from HIV, murine leukemia virus and VSV have been shown to be co-packaged with EBOV-GP into retrovirus pseudotype particles because the viral GPs were recruited to the same assembly and budding sites at the plasma membrane (51). Interestingly, the poxvirus glycoprotein B5 was not detected in EBOV-VLPs in our study. Although B5 is able to reach the plasma membrane of vaccinia virus infected cells, it is actively retrieved from the cell surface and redirected to the Golgi compartment (39), where wrapping of mature poxviral particles with additional membranes takes place (52,53). Hence, poxviral and filoviral membrane-associated proteins accumulate and assemble at distinct cellular membrane compartments which explains why B5 is absent from EBOV-VLPs that were released from MVA-EBOV-VLP infected cells.

The NP of filoviruses has been shown to accumulate in cytoplasmic inclusion bodies forming densely packed helical structures with a diameter of 20 - 25 nm (43,54). Using confocal immunofluorescence analysis, we observed similar inclusion bodies in cells infected with MVA-BN-EBOV-VLP or following transfection of cells with plasmids encoding EBOV-VP40 and EBOV-NP. These inclusion bodies were intensely stained with antibodies specifically reacting with the respective NP (Fig. 2 and data not shown). In addition, ultrathin sections of MVA-BN-

EBOV-VLP infected cells contained large aggregates consisting of nucleocapsid-like helical structures (data not shown). In contrast to some published reports (18,37), we did not observe redistribution of the homologous EBOV-NP from inclusion bodies to sites of EBOV-VP40 accumulation at the plasma membrane when MVA infected cells were co-transfected with plasmids encoding EBOV-NP and EBOV-VP40 (data not shown). In addition, cells infected with MVA-BN-EBOV-VLP also showed large inclusion bodies consisting of NP (Fig. 2) similar to what has been reported for EBOV infected as well as MARV infected cells (54,55). Using a purely plasmid-driven system, Hoenen et al. also observed that inclusion bodies formed by NP in human Huh-7 cells remained stable when VP40 was co-expressed, and that rather some VP40 was associated with the NP inclusion bodies (56). We therefore assume that the complete resolution of the large NP inclusion bodies might require very strong VP40 expression that is apparently neither achieved in natural infection nor in most expression systems including ours. The fact that we did not observe resolution of NP inclusion bodies by VP40 co-expression does not exclude NP-VP40 interactions between a fraction of VP40 and NP molecules. Such interactions did apparently occur as evidenced by the incorporation of TAFV-NP as well as EBOV-NP into MVA-driven EBOV-VLPs (Fig. 3, 5) as well as by the productive infection of cells with EBOV and MARV despite persistence of NP inclusion bodies.

VP40 is a major player in filovirus budding and VLP formation (12-15). Even if VLP formation is triggered by VP40 of MARV, i.e. a virus from a different filoviral genus, EBOV-GP is efficiently incorporated into VLPs (57). This finding is most likely attributable to the fact that a direct interaction of GP and VP40 is not required for GP incorporation into VLPs. Rather, GP is targeted to the same lipid raft domains that VP40 associates with (12,58,59). It has been shown in co-transfection experiments that EBOV-NP enhances the efficacy of homologous EBOV-VP40-driven VLP formation and that it is incorporated into VLPs independently of GP (18,19). Incorporation of the RNP complex, of which NP is a major component, has been shown to occur in a genus-specific manner (60).

There is also evidence that NP and VP40 directly interact via both C-terminal and N-terminal domains of NP, with the C-terminus being most critical for packaging of nucleocapsids into EBOV particles (37,60). Since the NP amino acid sequences differ by at least 30% between ebolavirus species and sequence variations are most pronounced at the C-terminus, it was unclear whether packaging of a heterologous NP from a different ebolavirus species would occur. In the MVA-BN-EBOV-VLP construct investigated here, the gene encoding the heterologous TAFV-NP had been inserted to broaden the species coverage of the vaccine construct with respect to cellular immune responses. Our data suggest that both the heterologous TAFV-NP and the homologous EBOV-NP were able to enhance VLP formation (Fig. 3, 5). Western blot analyses suggested that both NPs were present in VLPs, whereas definite ring-like nucleocapsid structures in VLP cross-sections could only clearly be discerned by EM analysis when EBOV-NP was used (Fig. 6). Direct comparison of the EBOV-NP or TAFV-NP expression levels and presence in VLPs by Western blot was not feasible because different antibodies were required for detection. However, EGFP marker analysis and qPCR data indicated similar cellular expression levels of NPs. It will be of interest to determine whether the formation of nucleocapsid-like structures by TAFV-NP and EBOV-NP requires different viral cofactors, or whether TAFV nucleocapsids are morphologically distinct from EBOV nucleocapsids.

The immune correlates of vaccine-induced protection against EVD are still not well defined, but multiple studies in NHPs as well as observations made with human EVD patients indicate that antibodies are important in protection against EVD (17,61). We therefore determined antibody responses induced by the MVA-BN-EBOV-VLP vaccine in mice (Fig. 7). Our basic analysis indicated that there was no significant difference in the amount of GP-specific binding or neutralizing antibodies or GP-specific IgG1/IgG2a isotype ratio induced by MVA-BN-EBOV-VLP compared to MVA-BN-EBOV-GP. However, the advantage of the VLP approach might reside in the quality of the vaccine antigen and thus the quality of the antibody response. Antibodies may

protect from EVD by directly neutralizing the virus, but non-neutralizing antibodies can also be protective (62). One potential mechanism of protection by non-neutralizing antibodies may rely on the inhibition of filovirus particle release from cells (63). NK cell-mediated antibody-dependent cellular cytolysis (ADCC), complement-mediated cell lysis and macrophage-mediated antibody-dependent cellular phagocytosis (ADCP) might also contribute to protection by antibodies. Furthermore, mice are not known as natural hosts for filoviruses and the quality and quantity of antibodies induced by MVA-BN-EBOV-VLP in primates may show greater differences to those induced by MVA-BN-EBOV-GP than in mice. An investigation of the potential of MVA-BN-EBOV-VLP to induce antibodies that exert protective functions such as ADCC or ADCP is warranted.

CD8 T cell responses are thought to contribute to protection against EVD, and MVA is recognized as a potent inducer of CD8 T cell responses. We found that the frequencies of GP-specific CD8 T cells in the blood and in the spleen at different time points after immunization were very similar or possibly even somewhat lower in mice vaccinated with MVA-BN-EBOV-VLP compared to vaccination with MVA-BN-EBOV-GP (Fig. 8 and data not shown). This slightly lower GP-specific response might have occurred due to the strong expression by the MVA-BN-EBOV-VLP construct of two additional filoviral antigens, VP40 and NP, which are predicted to contain good CD8 T cell epitopes in the H-2k background. We did not attempt to define VP40- and NP-derived epitopes in this background, but should such immunogenic epitopes exist, it is conceivable that the CD8 T cell response against these antigens would compete with that against GP and would likely reduce the GP-specific response. A similar phenomenon was observed e.g. for the CD8 T cell response against the B8 MVA antigen that was reduced depending on the strength of early ovalbumine expression in the H-2b background (64). It is thus possible that the GP-specific CD8 T cell response induced by MVA-BN-EBOV-VLP might be similar or even higher without this competition effect compared to single GP expression. On

661 the other hand, the MVA-BN-EBOV-VLP vaccine construct could possibly induce a broader CD8
662 T cell response against filovirus antigens.
663 In summary, we found that the MVA vaccine vector allows efficient formation and release of
664 *bona fide* GP-spiked EBOV-VLPs and efficiently induces GP-specific antibody and T cell
665 responses. The MVA-filovirus VLP platform might be further armed with additional GP antigens
666 derived from different ebolavirus species as well as from MARV to ultimately generate a
667 multivalent and highly immunogenic pan-filovirus vaccine.
668
669

670 **Acknowledgments**
671 M.S., S.W., M.W., M.K., U.D., R.S., H.L., H.H., P.C. and J.H. are employees of Bavarian Nordic
672 GmbH, which is the funding corporation of this study. Mark Suter is a consultant to Bavarian
673 Nordic. P.C. is a shareholder of Bavarian Nordic.
674 We thank Jutta Kramer and Johannes Poddobrjanski for producing purified viral stocks,
675 Sebastian Kraus and Marlene Geiger for excellent technical assistance, and Yvonne Terkowski
676 and Christian Krause for their help with the animal experiments, all from Bavarian Nordic GmbH.

Figure legends

Figure 1

Cellular expression of ebolavirus GP, VP40 and NP driven by recombinant MVAs.

(A) Schematic representation of MVA wild-type (MVA-BN) and MVA recombinants expressing *Zaire ebolavirus* glycoprotein (EBOV-GP) either alone (MVA-EBOV-GP) or in combination with the EBOV matrix protein VP40 (EBOV-VP40) and the *Taï Forest ebolavirus* nucleoprotein (TAFV-NP) (MVA-BN-EBOV-VLP). Expression cassettes were introduced into the MVA genome at intergenic regions (IGRs) (indicated as black arrows). The poxviral promoters PrS and PrS5E driving gene transcription of filoviral transgenes are indicated. **(B, C, D)** HeLa cells in 12-well plates were infected with the indicated viruses at a multiplicity of infection (MOI) of 10. **(B)** For Western blot analysis, cells were lysed at 6 h and 24 h p.i. in 150 µl of 1x Laemmli sample loading buffer. Cellular lysates prepared at 24 h p.i. were diluted 1:3 as indicated (*), separated by reducing SDS-PAGE, and transferred to PVDF membranes. Blots were incubated with anti-GP antibody (mAb 6D8) and subsequently with anti-mouse IgG peroxidase conjugate. The immunoblots were developed with a standard chemiluminescent peroxidase substrate. **(C)** Analysis of N-glycosylation patterns of EBOV-GP. HeLa cells were lysed in 150 µl of 1x RIPA buffer at 17 h p.i. Protein lysates were treated with Endo H or PNGase F, or were left untreated (-). Following endoglycosidase treatment, the proteins were mixed with 3x Laemmli loading buffer, separated by reducing SDS-PAGE and analyzed by immunoblotting using an anti-GP antibody (mAb 6D8). The immunoblot was developed using an ECL detection system with enhanced sensitivity. **(D)** Flow cytometric analysis of EBOV-GP expression. At 4 h and 24 h p.i., HeLa cells were suspended in PBS/2% FCS and incubated with anti-EBOV-GP antibody (mAb 6D8) and subsequently with anti-mouse IgG-allophycocyanin. Stained cells were analyzed by flow cytometry; cell surface expression of EBOV-GP is represented in histogram plots. **(E)** HEK 293T/17 cells in 12-well plates were incubated for 2 h with the indicated viruses (MOI of 5). Thereafter, the inoculum was replaced with DMEM/2% FCS. One day after infection, adherent

cells were lysed in 1x Laemmli loading buffer and analyzed by immunoblotting using antibodies directed to EBOV-GP, EBOV-VP40 or TAFV-NP.

Figure 2

Intracellular distribution of EBOV-GP, EBOV-VP40 and TAFV-NP expressed by recombinant MVAs.

HeLa cells infected with MVA-BN-EBOV-VLP (expressing EBOV-GP, EBOV-VP40 and TAFV-NP), MVA-BN-EBOV-GP (expressing EBOV-GP alone) or MVA wt were fixed and permeabilized 6 h p.i. and incubated with either anti-EBOV-GP mAb 6D8 (green), polyclonal rabbit anti-EBOV-VP40 antibody (magenta) or with the polyclonal rabbit anti-TAFV-NP antibody (cyan). Antigen-bound primary antibodies were detected with Alexa Fluor-conjugated secondary antibodies and cells analyzed with an inverse confocal laser-scanning microscope. MVA vector infected cells were detected by either EGFP or RFP fluorescence (shown in grey).

Figure 3

Release of MVA-encoded EBOV-VLPs and incorporation of TAFV-NP.

293T/17 cells in T75 cell culture flasks were infected (MOI of 10) with MVA-BN-EBOV-VLP (expressing EBOV-GP, EBOV-VP40 and TAFV-NP), MVA-BN-EBOV-GP (expressing EBOV-GP alone) or MVA-BN wt. After two hours, the inoculum was replaced with DMEM/5% FCS. One day after infection, supernatants from infected cells were precleared (400 g for 5 min) and purified by centrifugation through a 20% sucrose cushion at 36,000 rpm in a Beckmann SW41 rotor for 2 h. The adherent cells were scraped in PBS and lysed in 1x Laemmli sample loading buffer. Cell lysates (CL), precleared supernatants (SN) and VLP preparations (VLP prep) were analyzed by immunoblotting using antibodies directed to either EBOV-GP, EBOV-VP40 or TAFV-NP. Western blot images were acquired using Kodak BioMax Light Films (Sigma-Aldrich, Munich, Germany).

Figure 4

Transmission electron microscopy (TEM) analysis of EBOV-VLPs in MVA-BN-EBOV-VLP infected cells and of concentrated VLP preparations.

(A, B) TEM analysis of ultrathin sections. HeLa cells were infected with MVA-BN-EBOV-VLP **(A)** or MVA-BN **(B)** using an MOI of 10 and fixed 1 d p.i. with glutaraldehyde and osmium tetroxide and embedded in Epon. Ultrathin sections were stained with uranyl-acetate and lead citrate and analyzed by TEM. Scale bars: 0.2 µm. **(C-H)** Immuno-EM analysis of concentrated VLP preparations from supernatants of HeLa cells infected for 24 h at a MOI of 10 with MVA-BN-EBOV-VLP **(C, F)**, MVA-BN-EBOV-GP **(D, G)** and MVA-BN **(E, H)**. **(C, D, E)** Samples were adsorbed to EM grids and incubated with anti-EBOV-GP mAb 6D8 and subsequently with secondary anti-mouse IgG antibody coupled to 18 nm colloidal gold. **(F, G, H)** Samples were adsorbed to EM grids and incubated with anti-EBOV-GP mAb 6D8 and polyclonal rabbit anti-vaccinia B5 antibody. The antigen-bound primary antibodies were detected with anti-mouse IgG conjugated with 12 nm colloidal gold and anti-rabbit IgG antibody conjugated with 18 nm colloidal gold.

Figure 5

Release of MVA-expressed EBOV-VLPs and incorporation of NP.

(A) HEK 293T/17 cells in 12-wells were infected with MVA-BN (MOI of 5) and subsequently transfected with plasmids encoding the indicated filoviral proteins under the control of a poxviral early/late promoter. After 17 h of infection/transfection, cell supernatants were filtered and concentrated using Amicon® Ultra 100K centrifugation columns according to the manufacturer's instructions. The adherent cells were lysed in 250 µl 1x Laemmli sample loading buffer. Cell lysates (CL) and Amicon column-purified supernatants (pur-SN) were analyzed by immunoblotting using antibodies directed to either TAFV-NP, EBOV-VP40 or EBOV-NP. For

detection of TAFV-NP (lower panel) a chemiluminescent substrate with enhanced sensitivity was used. **(B)** For analysis of B5 expression, cells were treated as described above, an uninfected mock control was included as control. Western blot of CLs and pur-SNs was probed with a polyclonal rabbit anti-vaccinia B5 antibody. All Western blots images were acquired using ChemiDoc Touch System, images were analyzed and signals quantified with Image Lab™ Software. The data shown are representative for at least three independent experiments.

Figure 6

Transmission EM analysis of transfected VLP-producing cells.

HeLa cells in 6-wells were infected with MVA-BN (MOI of 5) and subsequently transfected with plasmids encoding EBOV-VP40 and EBOV-NP **(A)** or EBOV-VP40 and TAFV-NP **(B)**. At 12 h p.i., cells were harvested by scraping and fixed with 2.5% glutaraldehyde. Thin sections of fixed cells were prepared and analyzed by transmission EM. **(A)** The boxed areas of the microphotograph shown at higher magnification. Arrowheads indicate VLPs with an inner nucleocapsid-like structure appearing as a central ring (“bull´s eye”). A cross-section through a cellular filopodium is marked with an arrow. **(B)** Open arrow-heads point to “empty” VLP cross-sections. Note that only VLPs clearly showing a dark outer boundary were exactly cut in the perpendicular plane and therefore can reveal an inner ring.

Figure 7

EBOV-GP-specific antibody responses in mice following immunization with MVA-BN-EBOV-VLP.

CBA/J mice (group size n=5) were immunized intramuscularly in the hind leg on days 0 and 28 with either MVA-BN-EBOV-GP (GP) or MVA-BN-EBOV-VLP (VLP). Serum was sampled on days 21, 42, and 56 and analyzed by plaque reduction neutralization test 50 (PRNT50) using recombinant VSV-EBOV-GP as surrogate virus **(A)** and for antigen-binding antibodies by

EBOV-GP-specific ELISA for total IgG **(B)**, IgG1 **(C)** and IgG2a **(D)**. Differences were not statistically significant. The PRNT and ELISA results shown are from one of two representative independent experiments. * = analysis of pooled serum from five mice.

Figure 8

EBOV-GP-specific CD8 T cell responses in mice following MVA-BN-EBOV-VLP immunization.

CBA/J mice (group size n=5) were immunized on days 0 and 28 with either MVA-BN-EBOV-GP (GP) or MVA-BN-EBOV-VLP (VLP) by the intramuscular (i.m.) or intravenous (i.v.) route. Mice were sacrificed at day 56 and spleen cell suspensions were re-stimulated *in vitro* with EBOV-GP-derived peptide (TELRTFSI). Cells were stained for expression of CD4, CD8, CD44 and CD107a, production of IFN-γ, TNF-α and IL-2 was analyzed after intracellular cytokine staining by flow cytometry. Percentages of CD8 T cells expressing CD107a, IFN-γ, TNF-α or IL-2 are shown on the left, geometric mean fluorescence intensities (GMFI) of the signal for CD107a, IFN-γ, TNF-α and IL-2 are shown on the right. * = $p < 0.05$ by unpaired two-tailed Student's t test.

References

1. **Groseth A, Feldmann H, Strong JE**. 2007. The ecology of Ebola virus. Trends Microbiol **15:**408-416.

2. **Rougeron V, Feldmann H, Grard G, Becker S, Leroy EM**. 2015. Ebola and Marburg haemorrhagic fever. J Clin Virol **64:**111-119.

3. **Kuhn JH, Becker S, Ebihara H, Geisbert TW, Johnson KM, Kawaoka Y, Lipkin WI, Negredo AI, Netesov SV, Nichol ST, Palacios G, Peters CJ, Tenorio A, Volchkov VE, Jahrling PB**. 2010. Proposal for a revised taxonomy of the family Filoviridae: classification, names of taxa and viruses, and virus abbreviations. Arch Virol **155:**2083-2103.

4. **Geisbert TW, Geisbert JB, Leung A, Daddario-DiCaprio KM, Hensley LE, Grolla A, Feldmann H**. 2009. Single-injection vaccine protects nonhuman primates against infection with marburg virus and three species of ebola virus. J Virol **83:**7296-7304.

5. **WHO response team**. 2016. After Ebola in West Africa - unpredictable risks, preventable epidemics. N Engl J Med **375:**587-596.

6. **Marzi A, Robertson SJ, Haddock E, Feldmann F, Hanley PW, Scott DP, Strong JE, Kobinger G, Best SM, Feldmann H**. 2015. VSV-EBOV rapidly protects macaques against infection with the 2014/15 Ebola virus outbreak strain. Science **349:**739-742.

7. **Milligan ID, Gibani MM, Sewell R, Clutterbuck EA, Campbell D, Plested E, Nuthall E, Voysey M, Silva-Reyes L, McElrath MJ, De Rosa SC, Frahm N, Cohen KW, Shukarev G, Orzabal N, van DW, Truyers C, Bachmayer N, Splinter D, Samy N, Pau MG, Schuitemaker H, Luhn K, Callendret B, Van HJ, Douoguih M, Ewer K, Angus B, Pollard AJ, Snape MD**. 2016. Safety and Immunogenicity of Novel Adenovirus Type 26- and Modified Vaccinia Ankara-Vectored Ebola Vaccines: A Randomized Clinical Trial. JAMA **315:**1610-1623.

8. **Sullivan NJ, Geisbert TW, Geisbert JB, Xu L, Yang ZY, Roederer M, Koup RA, Jahrling PB, Nabel GJ**. 2003. Accelerated vaccination for Ebola virus haemorrhagic fever in non-human primates. Nature **424:**681-684.

9. **Tapia MD, Sow SO, Lyke KE, Haidara FC, Diallo F, Doumbia M, Traore A, Coulibaly F, Kodio M, Onwuchekwa U, Sztein MB, Wahid R, Campbell JD, Kieny MP, Moorthy V, Imoukhuede EB, Rampling T, Roman F, De R, I, Bellamy AR, Dally L, Mbaya OT, Ploquin A, Zhou Y, Stanley DA, Bailer R, Koup RA, Roederer M, Ledgerwood J, Hill AV, Ballou WR, Sullivan N, Graham B, Levine MM**. 2016. Use of ChAd3-EBO-Z Ebola virus vaccine in Malian and US adults, and boosting of Malian adults with MVA-BN-Filo: a phase 1, single-blind, randomised trial, a phase 1b, open-label and double-blind, dose-escalation trial, and a nested, randomised, double-blind, placebo-controlled trial. Lancet Infect Dis **16:**31-42.

10. **Warfield KL and Aman MJ**. 2011. Advances in virus-like particle vaccines for filoviruses. J Infect Dis **204 Suppl 3:**S1053-S1059.

11. **Warfield KL, Swenson DL, Olinger GG, Kalina WV, Aman MJ, Bavari S**. 2007. Ebola virus-like particle-based vaccine protects nonhuman primates against lethal Ebola virus challenge. J Infect Dis **196 Suppl 2:**S430-S437.

12. **Bavari S, Bosio CM, Wiegand E, Ruthel G, Will AB, Geisbert TW, Hevey M, Schmaljohn C, Schmaljohn A, Aman MJ**. 2002. Lipid raft microdomains: a gateway for compartmentalized trafficking of Ebola and Marburg viruses. J Exp Med **195:**593-602.

13. **Harty RN, Brown ME, Wang G, Huibregtse J, Hayes FP**. 2000. A PPxY motif within the VP40 protein of Ebola virus interacts physically and functionally with a ubiquitin ligase: implications for filovirus budding. Proc Natl Acad Sci U S A **97:**13871-13876.

14. **Jasenosky LD, Neumann G, Lukashevich I, Kawaoka Y**. 2001. Ebola virus VP40-induced particle formation and association with the lipid bilayer. J Virol **75:**5205-5214.

15. **Noda T, Sagara H, Suzuki E, Takada A, Kida H, Kawaoka Y**. 2002. Ebola virus VP40 drives the formation of virus-like filamentous particles along with GP. J Virol **76:**4855-4865.

16. **Falzarano D, Geisbert TW, Feldmann H**. 2011. Progress in filovirus vaccine development: evaluating the potential for clinical use. Expert Rev Vaccines **10:**63-77.

17. **Sullivan NJ, Martin JE, Graham BS, Nabel GJ**. 2009. Correlates of protective immunity for Ebola vaccines: implications for regulatory approval by the animal rule. Nat Rev Microbiol **7:**393-400.

18. **Kallstrom G, Warfield KL, Swenson DL, Mort S, Panchal RG, Ruthel G, Bavari S, Aman MJ**. 2005. Analysis of Ebola virus and VLP release using an immunocapture assay. J Virol Methods **127:**1-9.

19. **Licata JM, Johnson RF, Han Z, Harty RN**. 2004. Contribution of ebola virus glycoprotein, nucleoprotein, and VP24 to budding of VP40 virus-like particles. J Virol **78:**7344-7351.

20. **Mayr A, Stickl H, Müller HK, Danner K, Singer H**. 1978. [The smallpox vaccination strain MVA: marker, genetic structure, experience gained with the parenteral vaccination and behavior in organisms with a debilitated defence mechanism (author's transl)]. Zentralbl Bakteriol [B] **167:**375-390.

21. **Suter M, Meisinger-Henschel C, Tzatzaris M, Hülsemann V, Lukassen S, Wulff NH, Hausmann J, Howley P, Chaplin P**. 2009. Modified vaccinia Ankara strains with identical coding sequences actually represent complex mixtures of viruses that determine the biological properties of each strain. Vaccine **27:**7442-7450.

22. **Gomez CE, Najera JL, Krupa M, Perdiguero B, Esteban M**. 2011. MVA and NYVAC as vaccines against emergent infectious diseases and cancer. Curr Gene Ther **11:**189-217.

23. **Sutter G and Staib C**. 2003. Vaccinia vectors as candidate vaccines: the development of modified vaccinia virus Ankara for antigen delivery. Curr Drug Targets Infect Disord **3:**263-271.

24. **Meisinger-Henschel C, Späth M, Lukassen S, Wolferstätter M, Kachelriess H, Baur K, Dirmeier U, Wagner M, Chaplin P, Suter M, Hausmann J**. 2010. Introduction of the six major genomic deletions of modified vaccinia virus Ankara (MVA) into the parental vaccinia virus is not sufficient to reproduce an MVA-like phenotype in cell culture and in mice. J Virol **84:**9907-9919.

25. **Meisinger-Henschel C, Schmidt M, Lukassen S, Linke B, Krause L, Konietzny S, Goesmann A, Howley P, Chaplin P, Suter M, Hausmann J**. 2007. Genomic sequence of chorioallantois vaccinia virus Ankara, the ancestor of modified vaccinia virus Ankara. J Gen Virol **88:**3249-3259.

26. **Falkner FG and Moss B**. 1990. Transient dominant selection of recombinant vaccinia viruses. J Virol **64:**3108-3111.

27. **Chakrabarti S, Sisler JR, Moss B**. 1997. Compact, synthetic, vaccinia virus early/late promoter for protein expression. Biotechniques **23:**1094-1097.

28. **Wennier ST, Brinkmann K, Steinhäußer C, Mayländer N, Mnich C, Wielert U, Dirmeier U, Hausmann J, Chaplin P, Steigerwald R**. 2013. A novel naturally occurring tandem promoter in modified vaccinia virus Ankara drives very early gene expression and potent immune responses. PLoS ONE **8:**e73511.

29. **Kalhoro NH, Veits J, Rautenschlein S, Zimmer G**. 2009. A recombinant vesicular stomatitis virus replicon vaccine protects chickens from highly pathogenic avian influenza virus (H7N1). Vaccine **27:**1174-1183.

30. **Hoffmann M, Wu YJ, Gerber M, Berger-Rentsch M, Heimrich B, Schwemmle M, Zimmer G**. 2010. Fusion-active glycoprotein G mediates the cytotoxicity of vesicular stomatitis virus M mutants lacking host shut-off activity. J Gen Virol **91:**2782-2793.

31. **Schweneker M, Lukassen S, Späth M, Wolferstätter M, Babel E, Brinkmann K, Wielert U, Chaplin P, Suter M, Hausmann J**. 2012. The vaccinia virus O1 protein is required for sustained activation of extracellular signal-regulated kinase 1/2 and promotes viral virulence. J Virol **86:**2323-2336.

32. **Wolferstätter M, Schweneker M, Späth M, Lukassen S, Klingenberg M, Brinkmann K, Wielert U, Lauterbach H, Hochrein H, Chaplin P, Suter M, Hausmann J**. 2014. Recombinant modified vaccinia virus ankara generating excess early double-stranded RNA transiently activates protein kinase R and triggers enhanced innate immune responses. J Virol **88:**14396-14411.

33. **Meier AF, Laimbacher AS, Ackermann M**. 2016. Polycistronic Herpesvirus Amplicon Vectors for Veterinary Vaccine Development. Methods Mol Biol **1349:**201-224.

34. **Jeffers SA, Sanders DA, Sanchez A**. 2002. Covalent modifications of the ebola virus glycoprotein. J Virol **76:**12463-12472.

35. **Volchkov VE, Feldmann H, Volchkova VA, Klenk HD**. 1998. Processing of the Ebola virus glycoprotein by the proprotein convertase furin. Proc Natl Acad Sci U S A **95:**5762-5767.

36. **Volchkov VE, Volchkova VA, Slenczka W, Klenk HD, Feldmann H**. 1998. Release of viral glycoproteins during Ebola virus infection. Virology **245:**110-119.

37. **Noda T, Watanabe S, Sagara H, Kawaoka Y**. 2007. Mapping of the VP40-binding regions of the nucleoprotein of Ebola virus. J Virol **81:**3554-3562.

38. **McCarthy SE, Johnson RF, Zhang YA, Sunyer JO, Harty RN**. 2007. Role for amino acids 212KLR214 of Ebola virus VP40 in assembly and budding. J Virol **81:**11452-11460.

39. **Ward BM and Moss B**. 2000. Golgi network targeting and plasma membrane internalization signals in vaccinia virus B5R envelope protein. J Virol **74:**3771-3780.

40. **Spurgers KB, Alefantis T, Peyser BD, Ruthel GT, Bergeron AA, Costantino JA, Enterlein S, Kota KP, Boltz RC, Aman MJ, Delvecchio VG, Bavari S**. 2010. Identification of essential filovirion-associated host factors by serial proteomic analysis and RNAi screen. Mol Cell Proteomics **9:**2690-2703.

41. **Yasuda J, Nakao M, Kawaoka Y, Shida H**. 2003. Nedd4 regulates egress of Ebola virus-like particles from host cells. J Virol **77:**9987-9992.

42. **Johnson RF, Bell P, Harty RN**. 2006. Effect of Ebola virus proteins GP, NP and VP35 on VP40 VLP morphology. Virol J **3:**31.

43. **Noda T, Ebihara H, Muramoto Y, Fujii K, Takada A, Sagara H, Kim JH, Kida H, Feldmann H, Kawaoka Y**. 2006. Assembly and budding of Ebolavirus. PLoS Pathog **2:**e99.

44. **Spehner D and Drillien R**. 2008. Extracellular vesicles containing virus-encoded membrane proteins are a byproduct of infection with modified vaccinia virus Ankara. Virus Res **137:**129-136.

45. **Kushnir N, Streatfield SJ, Yusibov V**. 2012. Virus-like particles as a highly efficient vaccine platform: diversity of targets and production systems and advances in clinical development. Vaccine **31:**58-83.

46. **Swenson DL, Warfield KL, Larsen T, Alves DA, Coberley SS, Bavari S**. 2008. Monovalent virus-like particle vaccine protects guinea pigs and nonhuman primates against infection with multiple Marburg viruses. Expert Rev Vaccines **7:**417-429.

47. **Warfield KL, Bosio CM, Welcher BC, Deal EM, Mohamadzadeh M, Schmaljohn A, Aman MJ, Bavari S**. 2003. Ebola virus-like particles protect from lethal Ebola virus infection. Proc Natl Acad Sci U S A **100:**15889-15894.

48. **Warfield KL, Swenson DL, Negley DL, Schmaljohn AL, Aman MJ, Bavari S**. 2004. Marburg virus-like particles protect guinea pigs from lethal Marburg virus infection. Vaccine **22:**3495-3502.

49. **Warfield KL, Dye JM, Wells JB, Unfer RC, Holtsberg FW, Shulenin S, Vu H, Swenson DL, Bavari S, Aman MJ**. 2015. Homologous and heterologous protection of nonhuman primates by Ebola and Sudan virus-like particles. PLoS ONE **10:**e0118881.

50. **Sänger C, Mühlberger E, Klenk HD, Becker S**. 2001. Adverse effects of MVA-T7 on the transport of Marburg virus glycoprotein. J Virol Methods **91:**29-35.

51. **Gregory DA, Olinger GY, Lucas TM, Johnson MC**. 2014. Diverse viral glycoproteins as well as CD4 co-package into the same human immunodeficiency virus (HIV-1) particles. Retrovirology **11:**28.

52. **Blasco R and Moss B**. 1992. Role of cell-associated enveloped vaccinia virus in cell-to-cell spread. J Virol **66:**4170-4179.

53. **Smith GL and Law M**. 2004. The exit of vaccinia virus from infected cells. Virus Res **106:**189-197.

54. **Becker S, Rinne C, Hofsäss U, Klenk HD, Mühlberger E**. 1998. Interactions of Marburg virus nucleocapsid proteins. Virology **249:**406-417.

55. **Björndal AS, Szekely L, Elgh F**. 2003. Ebola virus infection inversely correlates with the overall expression levels of promyelocytic leukaemia (PML) protein in cultured cells. BMC Microbiol **3:**6.

56. **Hoenen T, Biedenkopf N, Zielecki F, Jung S, Groseth A, Feldmann H, Becker S**. 2010. Oligomerization of Ebola virus VP40 is essential for particle morphogenesis and regulation of viral transcription. J Virol **84:**7053-7063.

57. **Swenson DL, Warfield KL, Negley DL, Schmaljohn A, Aman MJ, Bavari S**. 2005. Virus-like particles exhibit potential as a pan-filovirus vaccine for both Ebola and Marburg viral infections. Vaccine **23:**3033-3042.

58. **Hoenen T, Volchkov V, Kolesnikova L, Mittler E, Timmins J, Ottmann M, Reynard O, Becker S, Weissenhorn W**. 2005. VP40 octamers are essential for Ebola virus replication. J Virol **79:**1898-1905.

59. **Panchal RG, Ruthel G, Kenny TA, Kallstrom GH, Lane D, Badie SS, Li L, Bavari S, Aman MJ**. 2003. In vivo oligomerization and raft localization of Ebola virus protein VP40 during vesicular budding. Proc Natl Acad Sci U S A **100:**15936-15941.

60. **Spiegelberg L, Wahl-Jensen V, Kolesnikova L, Feldmann H, Becker S, Hoenen T**. 2011. Genus-specific recruitment of filovirus ribonucleoprotein complexes into budding particles. J Gen Virol **92:**2900-2905.

61. **Marzi A, Engelmann F, Feldmann F, Haberthur K, Shupert WL, Brining D, Scott DP, Geisbert TW, Kawaoka Y, Katze MG, Feldmann H, Messaoudi I**. 2013. Antibodies are necessary for rVSV/ZEBOV-GP-mediated protection against lethal Ebola virus challenge in nonhuman primates. Proc Natl Acad Sci U S A **110:**1893-1898.

62. **Qiu X, Fernando L, Melito PL, Audet J, Feldmann H, Kobinger G, Alimonti JB, Jones SM**. 2012. Ebola GP-specific monoclonal antibodies protect mice and guinea pigs from lethal Ebola virus infection. PLoS Negl Trop Dis **6:**e1575.

63. **Kajihara M, Marzi A, Nakayama E, Noda T, Kuroda M, Manzoor R, Matsuno K, Feldmann H, Yoshida R, Kawaoka Y, Takada A**. 2012. Inhibition of Marburg virus

budding by nonneutralizing antibodies to the envelope glycoprotein. J Virol **86:**13467-13474.

64. **Baur K, Brinkmann K, Schweneker M, Pätzold J, Meisinger-Henschel C, Hermann J, Steigerwald R, Chaplin P, Suter M, Hausmann J**. 2010. Immediate-early expression of a recombinant antigen by modified vaccinia virus ankara breaks the immunodominance of strong vector-specific B8R antigen in acute and memory CD8 T-cell responses. J Virol **84:**8743-8752.

Figure 1

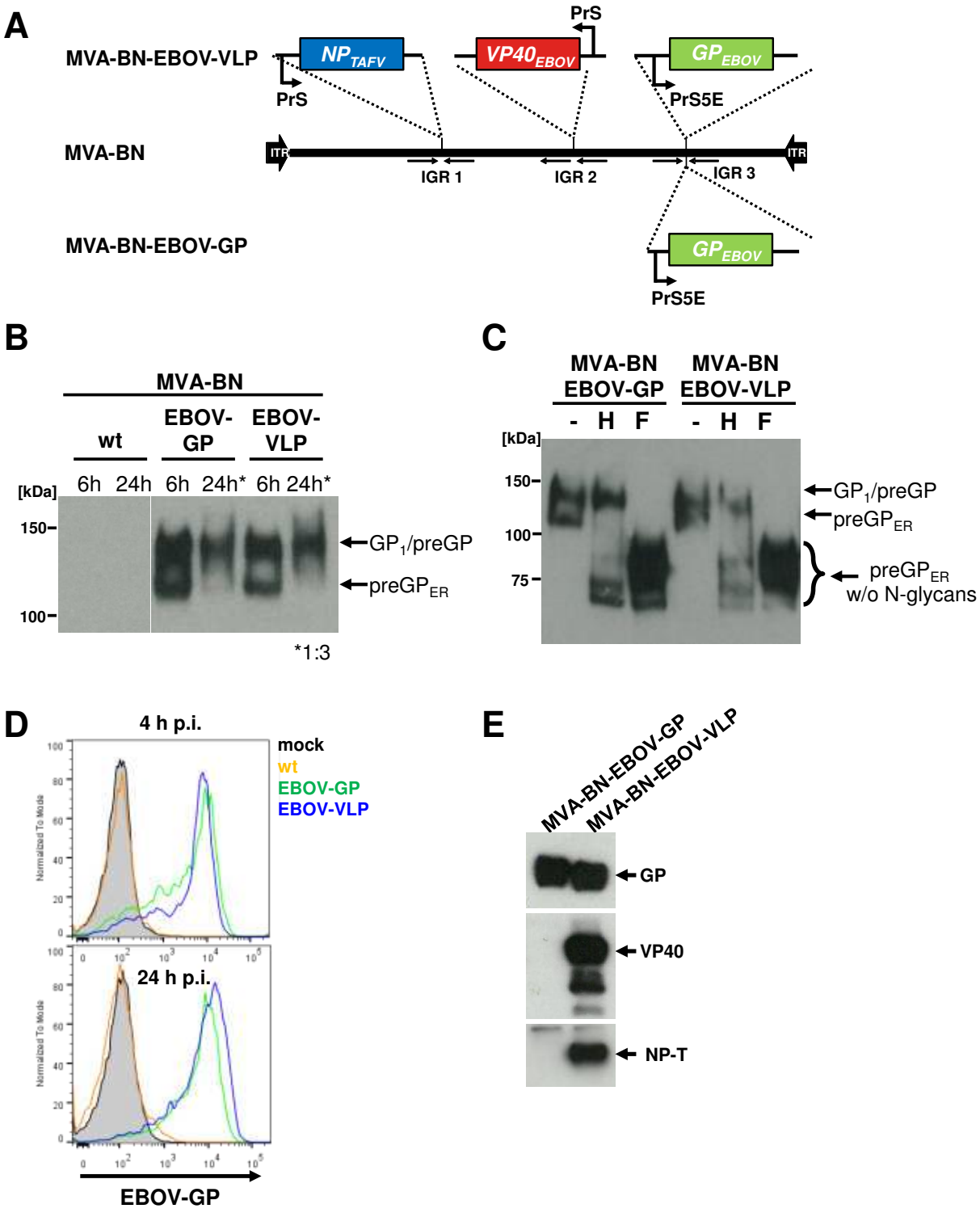

Figure 2

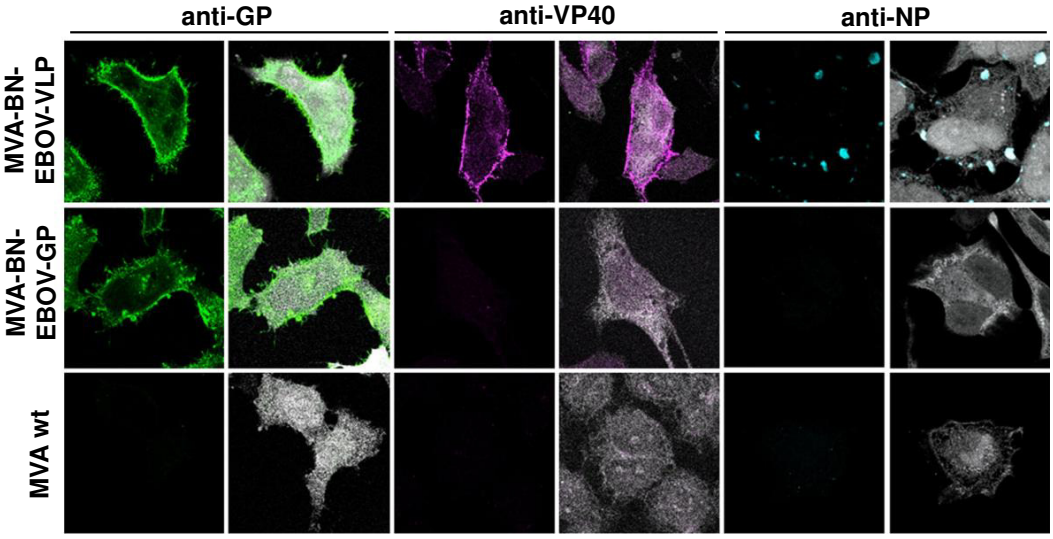

Figure 3

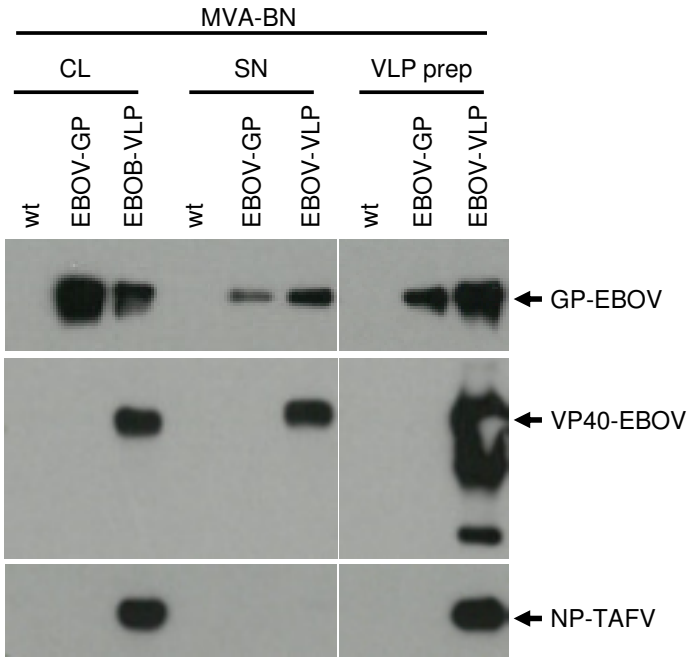

Figure 4

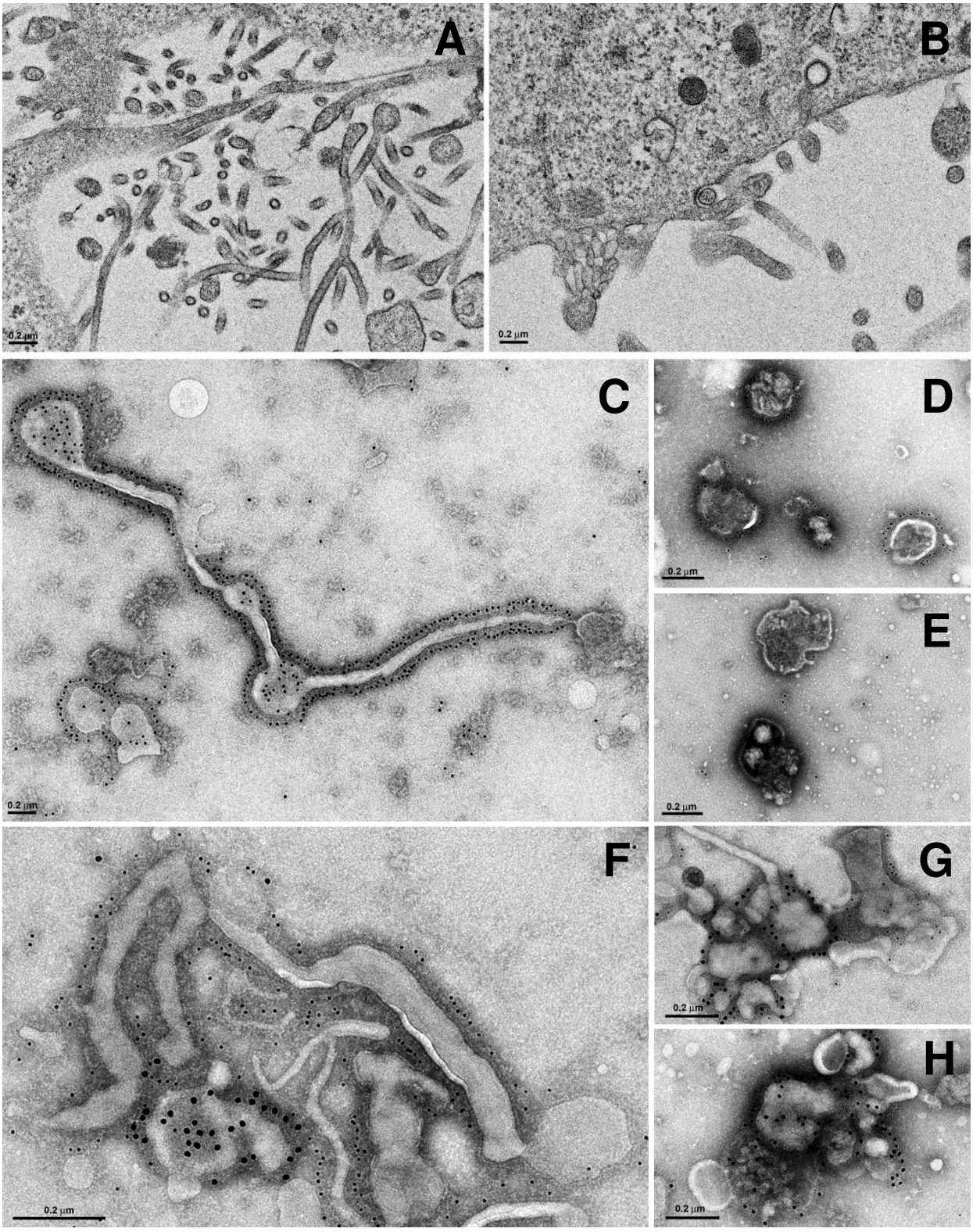

Figure 5

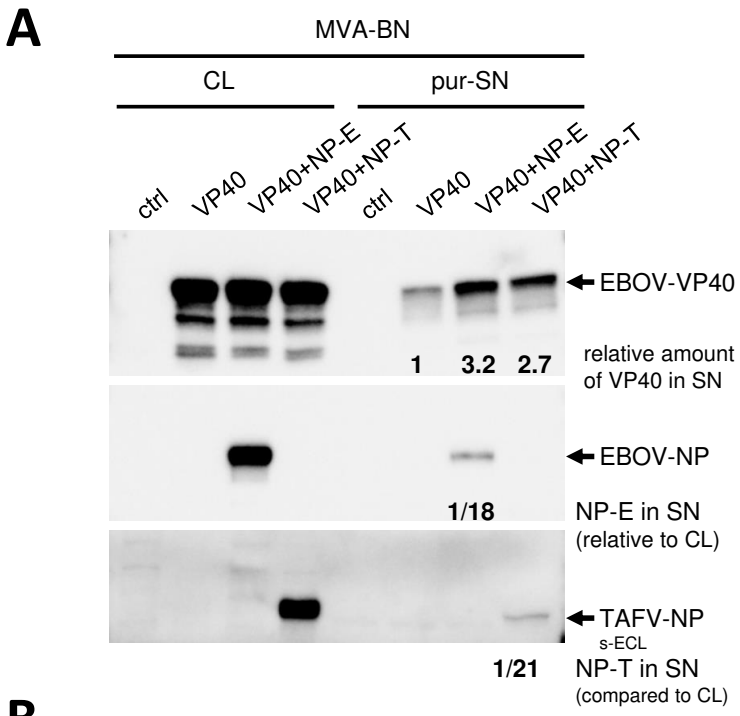

Figure 6

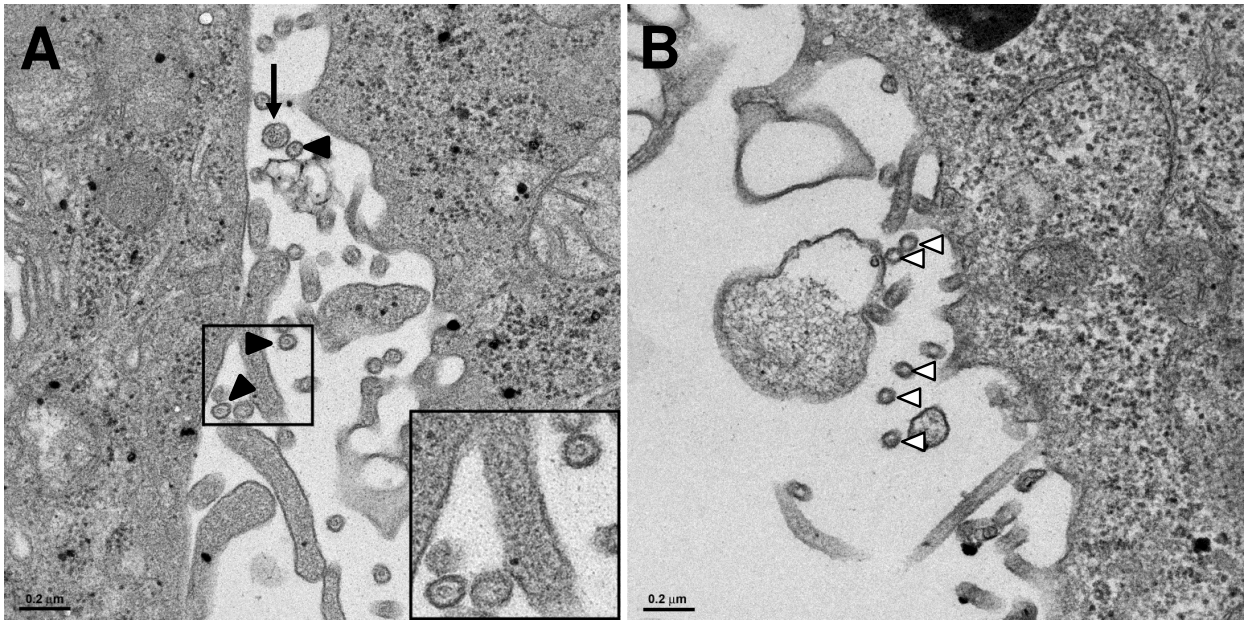

Figure 7

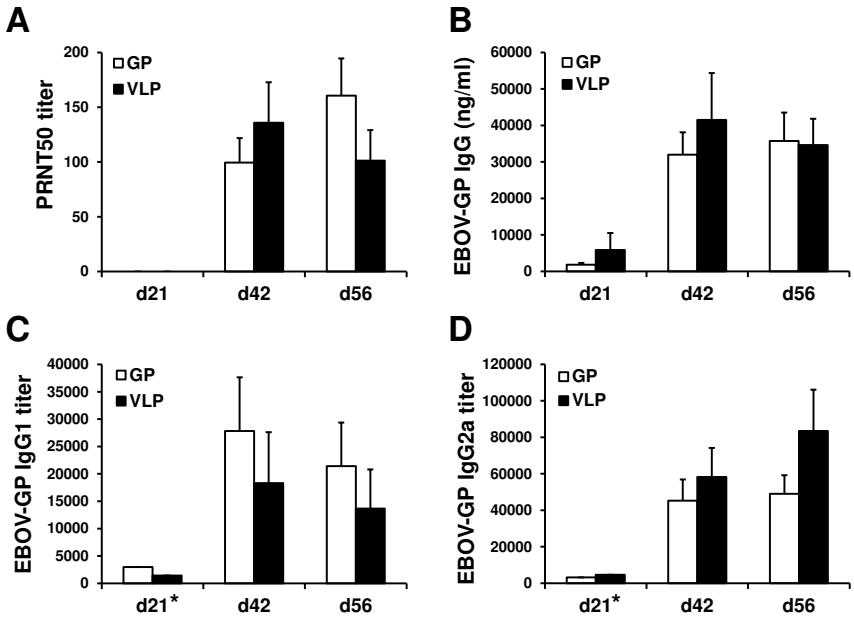

Figure 8